WEATHER CLIMATE WATER

WORLD METEOROLOGICAL ORGANIZATION | GLOBAL ATMOSPHERE WATCH

No. 8 – JULY 2024

WMO AIRBORNE DUST BULLETIN

Overview of global airborne dust in 2023

The global average of annual mean surface dust concentrations in 2023 (12.7 μg m^{-3}, see Figure 1(a)) was slightly lower than that in 2022 (13.8 μg m^{-3}, see *WMO Airborne Dust Bulletin, No. 7*). This decrease in 2023 is mainly attributed to reduced dust emissions from several dust-active regions around the world, such as North Africa, the Arabian Peninsula, the Iranian Plateau, northern India, central Australia and north-western China. But annual mean surface dust concentrations over western Central Asia, north-central China and southern Mongolia in 2023 were higher than those in 2022. Spatially, the estimated peak annual mean surface dust concentration (~800–1 100 μg m^{-3}) in 2023 was located in some areas of Chad in North-Central Africa. In the southern hemisphere, dust concentrations reached their highest level (~150–250 μg m^{-3}) in parts of central Australia and the west coast of South Africa. Wind-driven dust aerosols may be transported from these typical dust source areas to many regions worldwide over hundreds to thousands of kilometres. The regions that are most vulnerable to long-range transport of dust are the northern tropical Atlantic Ocean between West Africa and the Caribbean, South America, the Mediterranean Sea, the Arabian Sea, the Bay of Bengal and central-eastern China. In 2023, the transatlantic transport of African dust invaded parts of the Caribbean Sea region, and East Asian dust aerosols from the Gobi Desert also continued to reach the Bohai and Yellow Seas.

In the most affected areas, the annual mean surface dust concentration in 2023 was higher than the climatological mean. Exceptions to this were: most of West-Central Africa, including Senegal, the western Sahara, Guinea, Mauritania, Mali, Niger, Morocco, most of Algeria, Libya, south-central Chad and central Sudan; the Arabian Peninsula; the north of the Iranian Plateau; and mid-west Australia (Figure 1(b)). Hotspots with significantly higher dust concentrations were identified in South America; parts of North and Central Africa, including central and eastern Egypt, southern and northern Sudan, northern Chad, Liberia, Côte d'Ivoire, Ghana, Togo, Benin, western Nigeria, southern Cameroon, Gabon and Congo; the Red

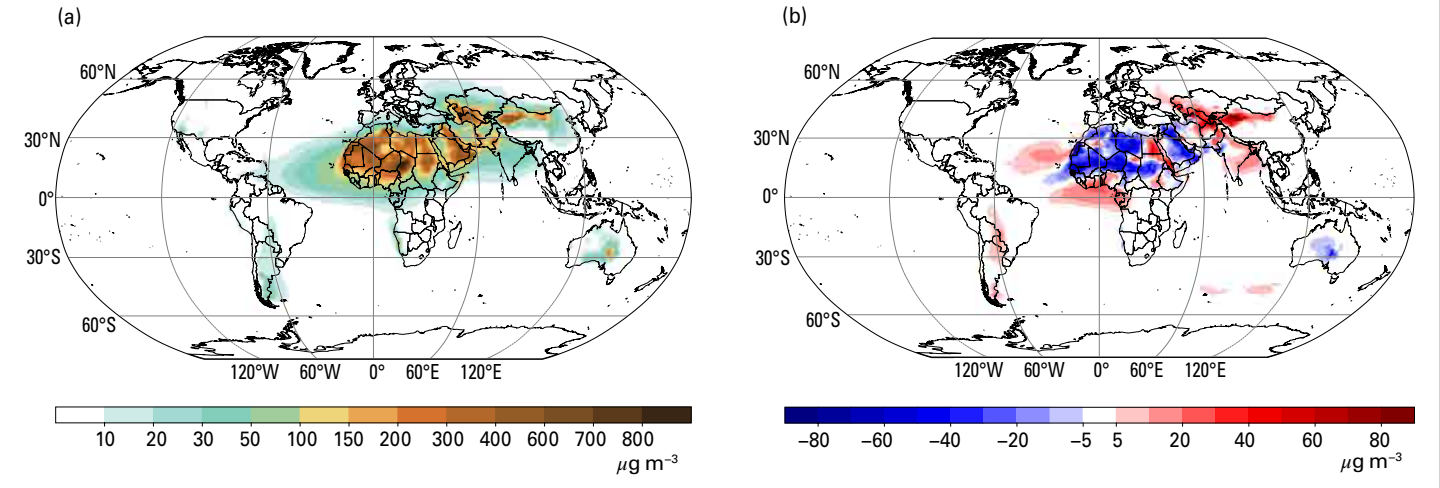

Figure 1. Annual mean surface concentration of mineral dust (in μg m^{-3}) in 2023. (b) Anomaly of the annual mean surface dust concentration in 2023 relative to the 1981–2010 mean.

Source: These results are derived from the Modern-Era Retrospective Analysis for Research and Applications, Version 2 (MERRA-2) (Gelaro et al., 2017)

Sea; the eastern Iranian Plateau; the Bay of Bengal; parts of Central Asia, including southern Kazakhstan, Iraq, Uzbekistan and Kyrgyzstan; South Asia; parts of East Asia, including north-west and north-central China, and the tropical Atlantic Ocean between West Africa and the Caribbean.

Severe dust storms over East Asia in spring 2023

The prolonged drought in the countries of the Asian region lasting more than a decade (*State of the Climate in Asia 2022*), along with the impact of other environmental factors, has created a crisis affecting natural resources and the environment in the region. The analysis of the surface dust concentration climatology in Figure 2 shows the highest dust concentrations (above 40 μg m^{-3}) between March and July in latitudes between 37°N and 43°N where the main deserts in Asia (the Gobi, Taklamakan and Karakum) are found. In latitudes between 27°N and 37°N there were moderate concentrations (above 30 μg m^{-3}) between April and September where the Thar desert in India and sources in the Sistan Basin of the Islamic Republic of Iran and the Tigris and Euphrates basin in Iraq are found.

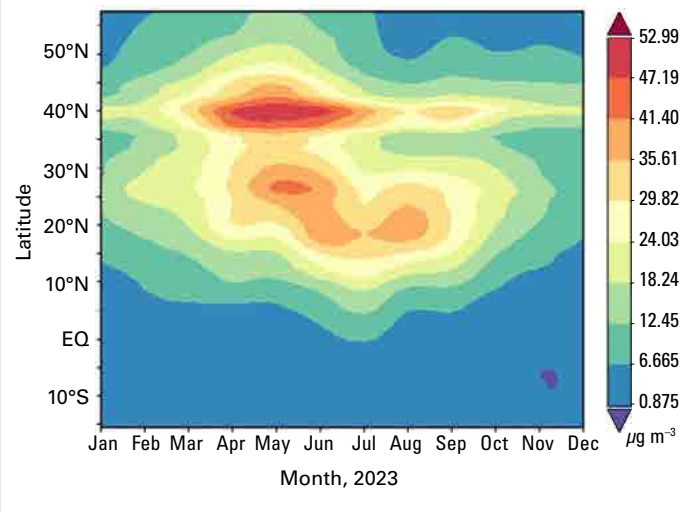

Figure 2. Monthly latitudinal surface dust concentration averages from January 2023 to December 2023 for the Asian region (10°S–50°N and 30°E–130°E)

Source: Data are based on the dust PM_{10} (particulate matter with diameter <10 μm) MERRA-2 reanalysis dataset from NASA (Gelaro et al., 2017)

March to May is the "dustiest" season in East Asia. In the spring of 2023, strong dust activity swept across the entire northern part of China as recorded by the air quality networks in the region (see PM_{10} mean annual values in Figure 3(a)), posing considerable challenges to public life and health. FY-4 satellites monitored 32 sand and dust storms (SDSs) in 2023, most of which (29 of the 32) occurred in the spring.

From the perspective of local surface conditions in dust sources, as shown in Liu et al. (2024), the spatial distribution of the surface air temperature during the preceding period (February–March–April) in the Gobi Desert shows evident warming, with an anomaly of approximately 1.5 °C compared to the mean state during 1991–2010. Furthermore, the precipitation and soil moisture both exhibit negative anomalies. These surface anomalies provided favourable conditions for the occurrence of dust activities in spring of 2023. Beyond the local surface considerations, the remote sea surface temperature (SST) anomalies can trigger large-scale atmospheric teleconnection through air–sea interactions, thereby changing the local wind speed and increasing the dust activity over northern China. In the North Atlantic, pronounced positive SST anomalies were observed in the spring of 2023 (Figure 3(b)).

An ongoing study examining the contributions of the deserts in Xinjiang, Mongolia and Inner Mongolia to dust in China, Japan and Republic of Korea during five dust

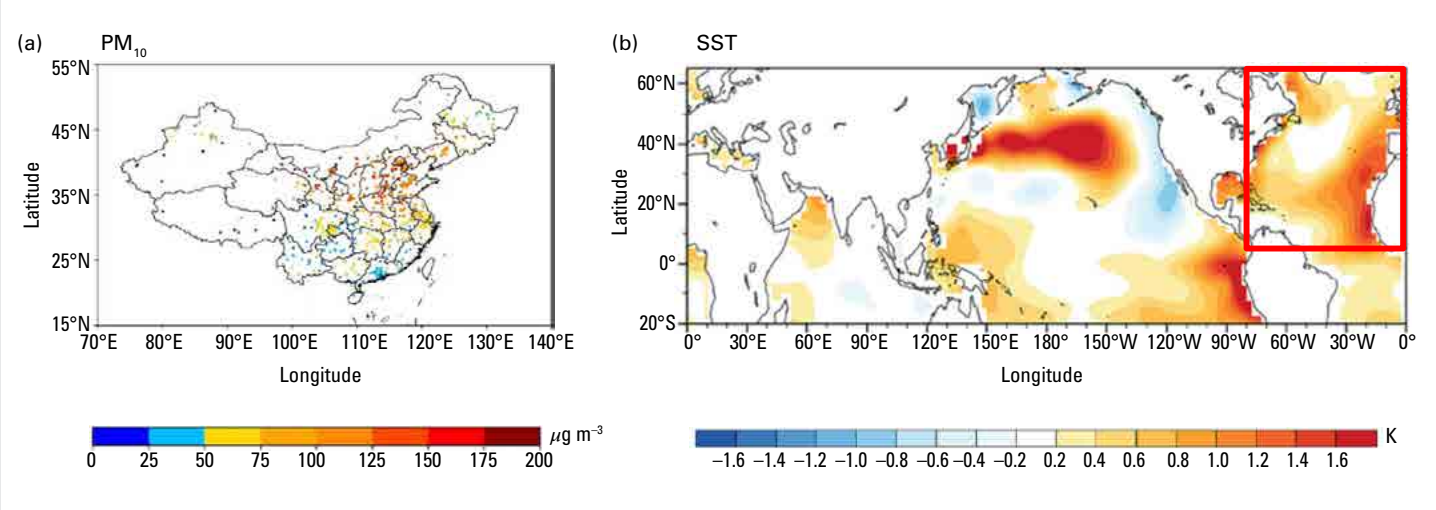

Figure 3. (a) Spring (March–April–May) mean of PM_{10} concentration in 2023 obtained from observing stations in China. (b) Sea surface temperature (SST) anomalies in spring of 2023 relative to 1991–2020 climate from ERA5.

Source: Adapted from Liu et al. (2024)

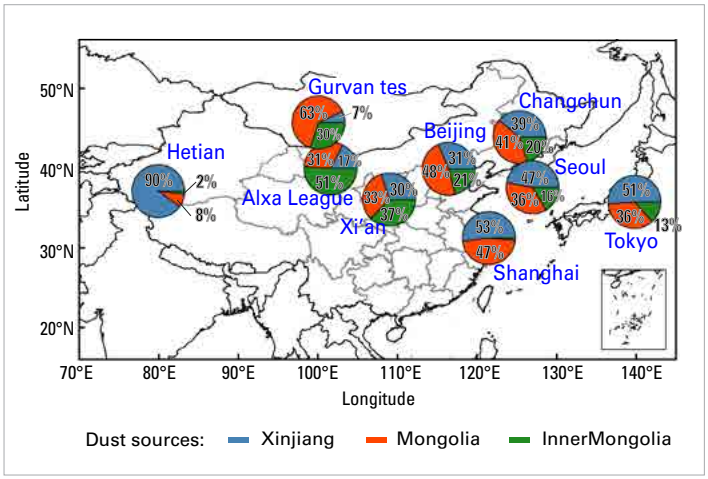

Figure 4. Contribution percentage of three deserts (those in Xinjiang, Mongolia and Inner Mongolia) to the surface dust concentration of the cities near the three deserts and downwind cities in China, Japan and Republic of Korea. The analysis considers five events that occurred in spring 2023: 9–12 March, 19–24 March, 9–15 April, 18–21 April and 18–21 May.

Source: Hong Wang

storms in spring 2023 (Figure 4) found that Xinjiang had the highest dust emissions, followed by Mongolia and Inner Mongolia. Contributions varied by city: Xinjiang mainly affected Hetian, Mongolia and Inner Mongolia influenced each other (Gurvan Tes and Alxa League), and all three impacted Xian. Mongolia had the largest impact on Beijing and Changchun, while Xinjiang was the primary contributor to dust in Shanghai, Seoul and Tokyo.

Major sand and dust storm events in 2023

Dust Harmattan surges over the Sahel and Gulf of Guinea in December

From 11 to 21 December 2023, several intense synoptic-scale dust outbreaks affected an extensive region of the western Maghreb, the Sahel and the Gulf of Guinea. Also, significant dust transport over the Atlantic could be observed during this event on the polar satellite imagery (Figure 5). Between 18 and 19 December, visibility dropped to 1 500 m in Sal (Cabo Verde) and Dakar (Senegal), 1 000 m in Bamako (Mali), 700 m in Nouakchott (Mauritania) (see dark brown circles in Figure 5, which indicate <1 km visibility). Multiple national meteorological agencies, such as the Agence Nationale de l'Aviation Civile et de la Météorologie of Senegal, issued warnings, and the media information highlighted the poor air quality (see, for example, https://expressodasilhas.cv/pais/2023/12/19/inmg-alerta-sobre-niveis-elevados-de-particulas-inalaveis-devido-a-bruma-seca/89172). The WMO Barcelona Dust Regional Center operational forecast system based on the MONARCH model correctly predicted this event.

Strong and persistent dust outbreaks attributed to Harmattan surges (HSs) began in the autumn of 2023 and recurred throughout the winter of 2023–2024 with significant impacts in the region. As in the situation described above, they were driven by a persistent zonal flux with numerous frontal systems and their associated upper-level troughs from the Atlantic over Europe, with some of them reaching Northern Africa. This pattern is a typical situation for HSs along with an intensification of the Libyan High. These HSs display a circulation pattern that is distinct from that associated with the sudden and severe dust outbreaks that impacted Northern Africa and Europe in previous years (Cuevas-Agulló et al., 2024). These earlier outbreaks were triggered by a combination of a cut-off low moving across North African latitudes and a blocking system over Europe.

Winter and early spring dust events in the eastern Caribbean and Northern South America

The boreal winter and early spring period of December 2023 to April 2024 saw a number of dust events affecting the eastern Caribbean and Northern South America (Copernicus Atmosphere Monitoring Service (CAMS)). The reference dust forecast system at the WMO Barbados Dust Regional Centre, WRF-Chem, managed by the Caribbean Institute for Meteorology and Hydrology (CIMH) (Figure 6), predicted the extent of the dust event in December 2023 which had its origin in the Sahara and hit the Caribbean on 25 December. This was confirmed

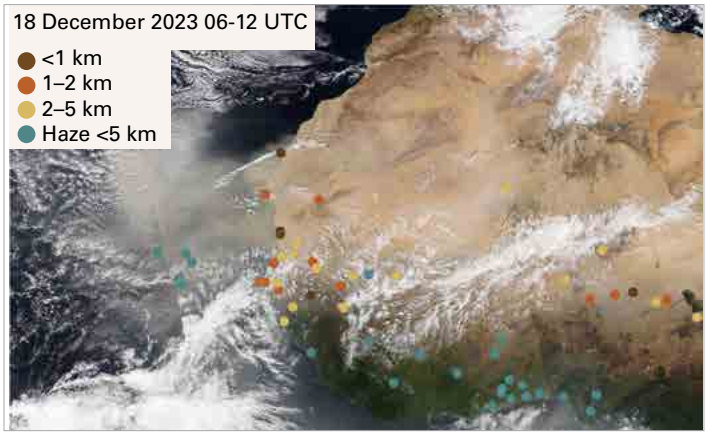

Figure 5. Visible image from the Visible Infrared Imaging Radiometer Suite (VIIRS) aboard the polar satellite NOAA-20 on 18 December 2024 and visibility reduction due to the presence of dust (coloured circles)

Sources: NASA Worldview and the WMO Barcelona Dust Regional Center

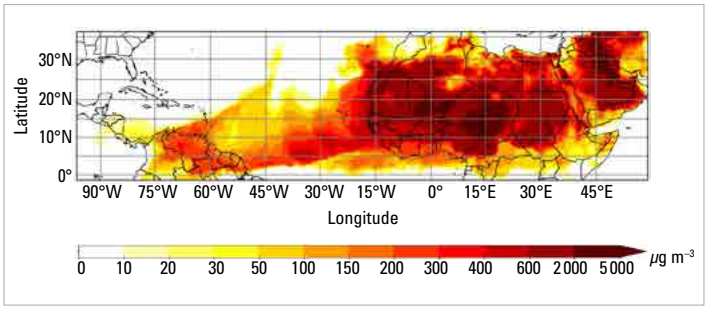

Figure 6. Seven-day surface dust concentration forecast valid 25 December 2023 at 0000 UTC

Source: Forecasts are based on the CIMH WRF-Chem system contribution to the WMO Barbados Dust Regional Centre

by an AERONET station in Barbados (Ragged Point station) that showed a maximum peak in aerosol optical depth (AOD) of 0.6 on 24 December (not shown here).

Dust events frequently impact the islands of Guadeloupe and Barbados (both in the eastern Caribbean) in summer, and occasional spring events impact Guadeloupe, Barbados and Cayenne, French Guiana (northern South America), as shown in Prospero et al. (2014). These recent winter–early spring dust events appear to be a variation to the climatological pattern that suggests a south-to-north progression of the most intense dust plume impacts on the Caribbean. Recent studies such as Zuidema et al. (2019) have suggested that intense dust events may be arriving earlier in the year for Barbados and, by extension, the eastern Caribbean.

Severe dust storms over East Asia in spring

During March to May 2023, East Asia was affected 13 times by intense dust intrusions. From 9 to 12 April 2023, due to the influence of a strong cyclone in Mongolia and the cold air behind it, a strong SDS occurred from southern Mongolia and affected most of China's Yangtze River, the Korean Peninsula, Japan and other areas moving eastwards towards the Pacific. The distribution map of maximum Infrared Difference Dust Index (IDDI) derived from FY-4 satellite (Figure 7) shows the strong SDS that occurred in most parts of the Mongolian Plateau on 10 April and was transported to north-east China during the following days. The air quality and visibility in these areas declined, with visibility reductions to <10 km (Figure 7(c)). Dust arrived on 12 April at most areas in northern and eastern Japan.

During the period of 19 to 24 March, the most severe SDS event of 2023 occurred, sweeping across Mongolia and northern China. The dust episode affected more than 4 million square kilometres, including 20 provinces in China. The event was triggered by a cyclone over Mongolia and intensified by a cold surface wind, leading to widespread sand lifting. The storm's progression from west to east resulted in a rapid spread of sand and dust, affecting Mongolia and China, and even reaching the Republic of Korea and Japan. The SDS episode caused a dramatic decline in air quality, with PM_{10} concentrations in some areas exceeding 9 000 μg m^{-3}. The severe SDS episode reduced visibility to less than 500 m in parts of Beijing and led to significant disruptions in transportation and daily life, highlighting the need for effective warning systems. Dust aerosols play a crucial role in climate forcing, which could modify the radiative balance of the Earth–atmosphere system by scattering or absorbing solar radiation and long-wave radiation from the surface to directly affect climate. Analyzing the dust radiative feedback using sensitive experiments, it has been shown that dust radiative feedback causes surface cooling in the eastern part of China. Notably, the reduction in temperature at 2 m could reach 0.4 °C. The extreme surface cooling caused by dust has had a serious impact on the public.

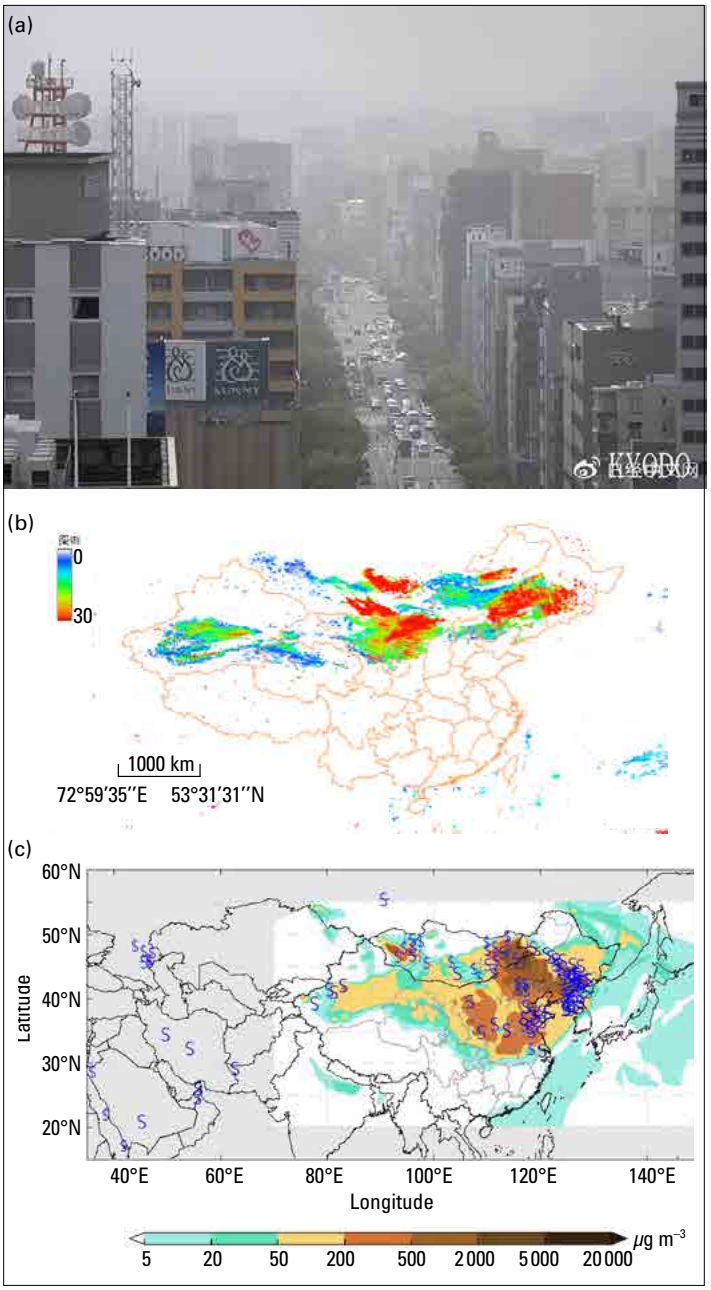

Figure 7. (a) Dust shrouded Fukuoka City (Japan) at 9:40 a.m. local time on 12 April. (b) The distribution map of maximum Infrared Difference Dust Index (IDDI) derived from FY-4 satellite for 10 April. (c) Comparison between observed SDS phenomenon and forecasted surface dust concentrations (μg m^{-3}) by ensemble forecast from the Sand and Dust Storm Warning Advisory and Assessment System (SDS-WAS) Asian Node at 0900 UTC on 11 April 2023. Blue symbols indicate the weather stations where dust was recorded.

Sources: (a) KYODO NEWS; (b) and (c) WMO Beijing Dust Forecast Center

Ongoing research

Towards better operational dust forecasts and predictions

Global ensemble dust forecasting

Forecasting dust events is fraught with uncertainties, since the forecasts are impacted by errors from the meteorological forecasts (for both emissions and

transport) and from the atmospheric composition forecasts (dust emission scheme, dust deposition), as well as possible errors regarding the inputs, such as the soil composition (between silt, sand and clay). All these errors will propagate through the dust forecast and will potentially also impact future forecasts, should the current forecast be used as initial conditions. An ensemble approach is well suited for quantifying these errors and how they propagate over time. In an ensemble of dust forecasts, stochastic perturbations are applied to initial conditions, inputs and model tendencies. This approach, long used for meteorological forecasts, can also be of use to better forecast extreme dust events and to provide a metric of how confident the model is in forecasting a dust event, through ensemble spread.

By combining the various kind of perturbations (that is, meteorological and chemistry initial conditions and tendencies, dust source function, soil type fractions, size distributions, anthropogenic emissions) the objective of this approach is to forecast and quantify the contribution of the meteorological uncertainties, of the dust input uncertainties and of the aerosol model uncertainties to the total uncertainty of the dust forecasts. Another objective is to investigate the potential added value of such an ensemble approach to the forecasting of dust storms.

Figure 8 shows an example of such an uncertainty analysis based on the experimental IFS-COMPO atmospheric composition ensemble with 50 perturbed members, designed by harnessing the work done to build the IFS numerical weather prediction (NWP) ensemble. A set of ensemble simulations that perturbed different combinations of the above factors were run for a dust event that struck large parts of western Europe between 20 and 22 February 2021. This analysis is preliminary, and valid only for this particular event over this specific region.

The results (Figure 8) allowed for a quantification of the uncertainty (as measured by ensemble spread) in simulated PM_{10} over a region encompassing Spain, France and the western Mediterranean. The aerosol initial conditions are the only source of uncertainty at forecast time 0 h, but its relative contribution quickly decreases with forecast time and becomes small beyond 48 h. Uncertainties associated with the simulated meteorology

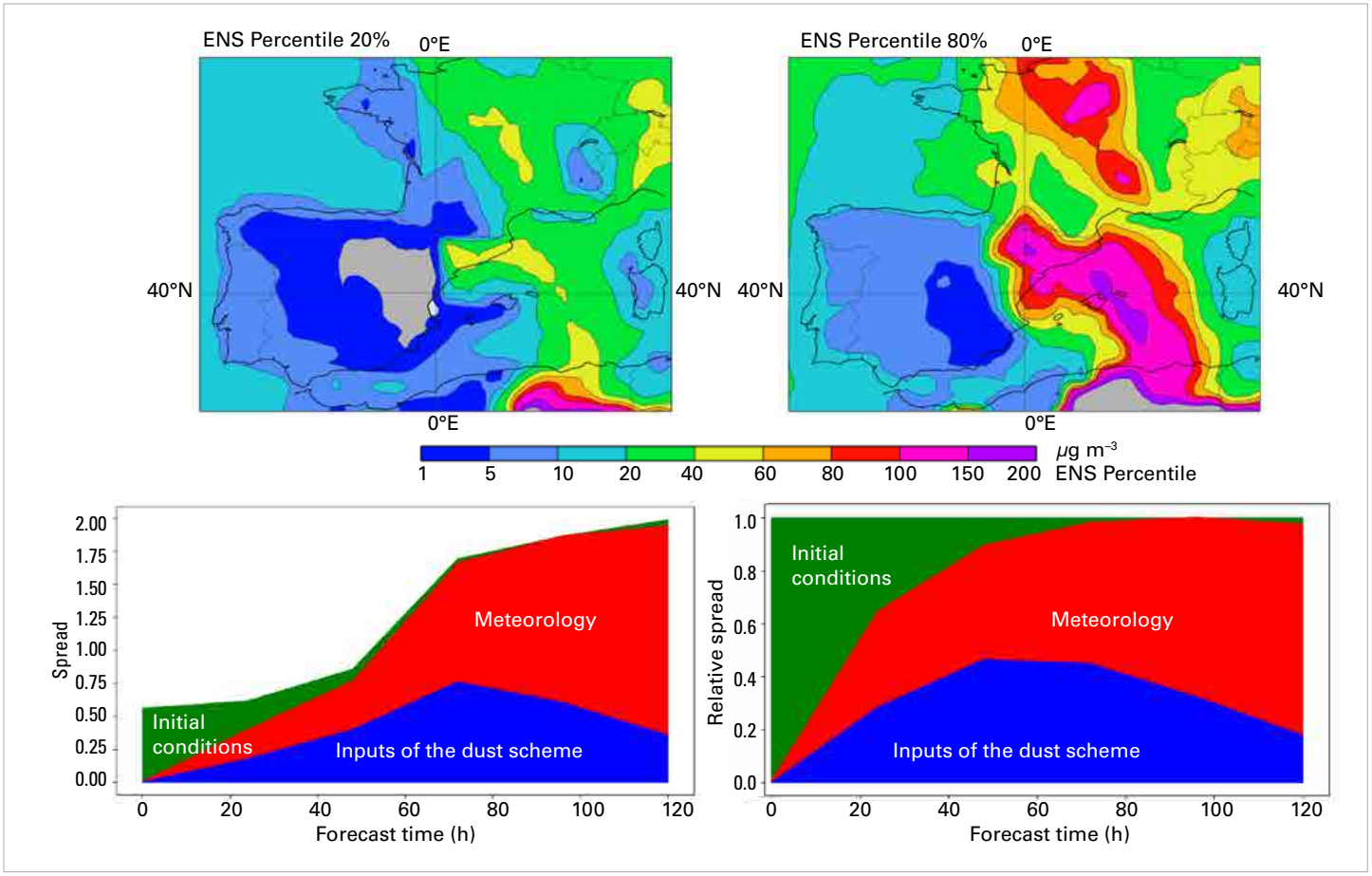

Figure 8. Top: Simulated PM_{10} on 21 February 2021 at 1200 UTC (84 h forecast), by an experimental IFS-COMPO ensemble simulation: 20th percentile (top left) and 80th percentile (top right). Bottom: Estimated sources of uncertainty of simulated PM_{10} as a function of forecast time evaluated by several IFS-COMPO ensemble simulations, for the region shown in the top panels and for a simulation starting on 19 February 2021 at 0000 UTC. The sources of uncertainty are aerosol initial conditions (green), meteorological uncertainties (red) and input of the dust scheme (blue). The absolute estimated uncertainty is shown in the bottom left panel, while the relative uncertainty for each source is shown on the right panel. The impact of anthropogenic emissions on the ensemble spread is small for this case study and is not shown.

grow with forecast time and become dominant after a forecast time of 72 h, representing 50% to 80% of total uncertainty for forecast times between 72 and 120 h. The uncertainties associated with the inputs of the dust scheme increase to a maximum value of 40% at forecast times between 48 and 72 h, at the peak of the simulated dust event, and then decrease to a value of 20% of uncertainty at a forecast time of 120 h.

Towards an operational regional dust assimilation system

Assimilation of satellite observations is now common in centres that provide global forecasts of mineral dust. Most of these centres assimilate observations from the Moderate Resolution Imaging Spectroradiometer (MODIS), which has delivered more than two decades of high-quality daily AOD retrievals. With the end of the MODIS mission now approaching (2026), most forecasting centres started assimilating observations from the Visible Infrared Imaging Radiometer Suite (VIIRS) instruments, which provide specifications similar to those of MODIS and are expected to operate well beyond 2030.

The reference forecast system at the WMO Barcelona Dust Regional Center is based on the MONARCH model. Among the ongoing efforts to improve the performance of MONARCH dust products, the assimilation of near-real-time VIIRS Deep Blue V2 aerosol retrievals (AOD550) from the NOAA-20 satellite is being tested. Following Escribano et al. (2022), the Local Ensemble Transform Kalman Filter (LETKF) is being tested with an ensemble of 12 MONARCH forecasts with perturbed dust emissions. All VIIRS AOD retrievals gathered over the simulation domain are first filtered for dust, based on the retrieval dust flag, and then averaged on a 10 km resolution grid. The assimilation produces a 24 h time series of corrected dust concentrations for the past day and an initial condition at 0000 UTC for the follow-up forecast. Once the model is initialized with a dust field that is in better agreement with satellite observations, a key question is how long assimilation corrections keep positively impacting the forecast. Figure 9 shows the average differences between VIIRS AOD and the model equivalent over North Africa, the Middle East and Europe during a 5-day testing period in January 2024 (data assimilation is performed only during the first three days). The plot shows that the impact of the VIIRS initialization is well measurable during the first day of forecast (DA-FCST D0); it rapidly fades after 24 h (DA-FCST D1) but still provides lower bias than the current operational forecast (OPER-FCST).

Daily assimilation of VIIRS observations is currently being deployed in pre-operational mode at the WMO Barcelona Dust Regional Center, with the objective of becoming fully operational in autumn 2024 and replacing the actual dust forecast.

Stone coverage effects

More than 50% of Earth's deserts are covered with stones, which suppress SDSs. Since dust particles influence climate change, studying these surfaces is crucial. For the first time, a SDS simulation scheme including a stony surface effect was tested by Sekiyama et al. (2023). The mathematical formulation of the stony surface effect was based on observations in East Asia and data from the SoilGrids 2.0 set. The meteorological and dust simulations were performed from 0000 UTC on 29 April 2017 to 0000 UTC on 7 May 2017. They reproduced fewer dust storms in areas with higher stone coverage and more in areas with lower coverage. This simulation result was consistent with SYNOP observations from

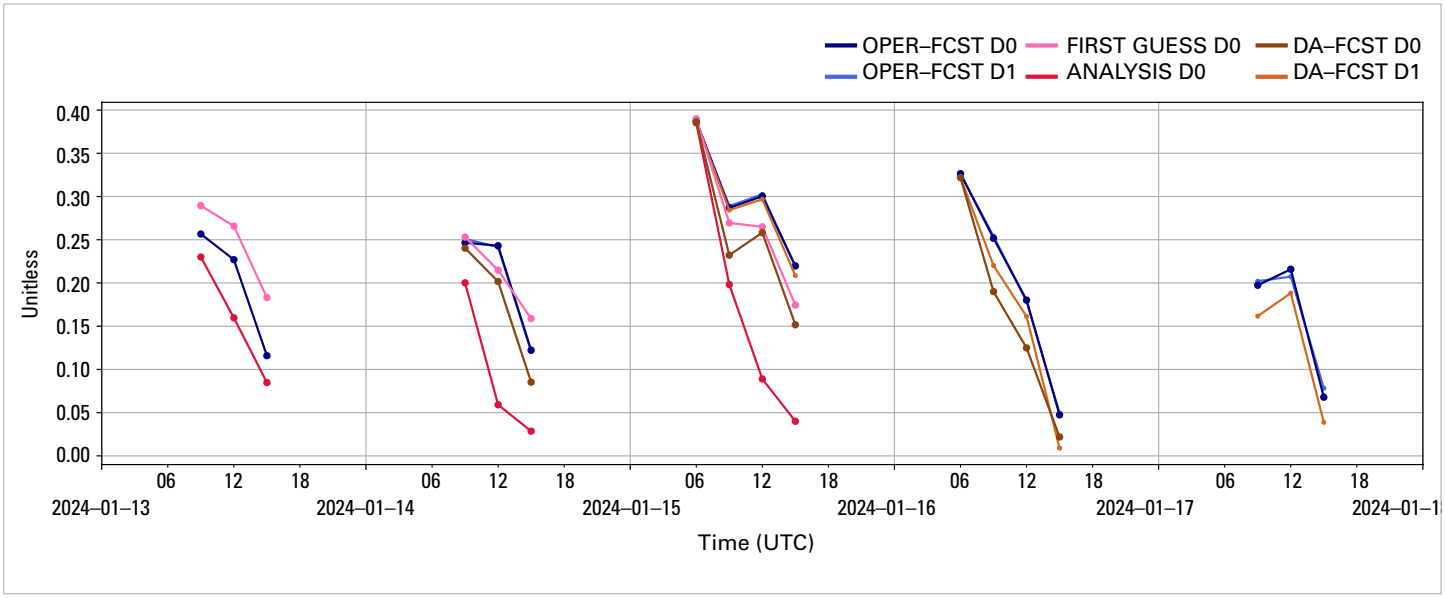

Figure 9. Average differences between VIIRS AOD at 550 nm and the model equivalent dust optical depth for the analysis (red), for different forecast lead times (D0 for a lead time <24 h, D1 for a lead time between 24 h and 48 h)

Source: MONARCH

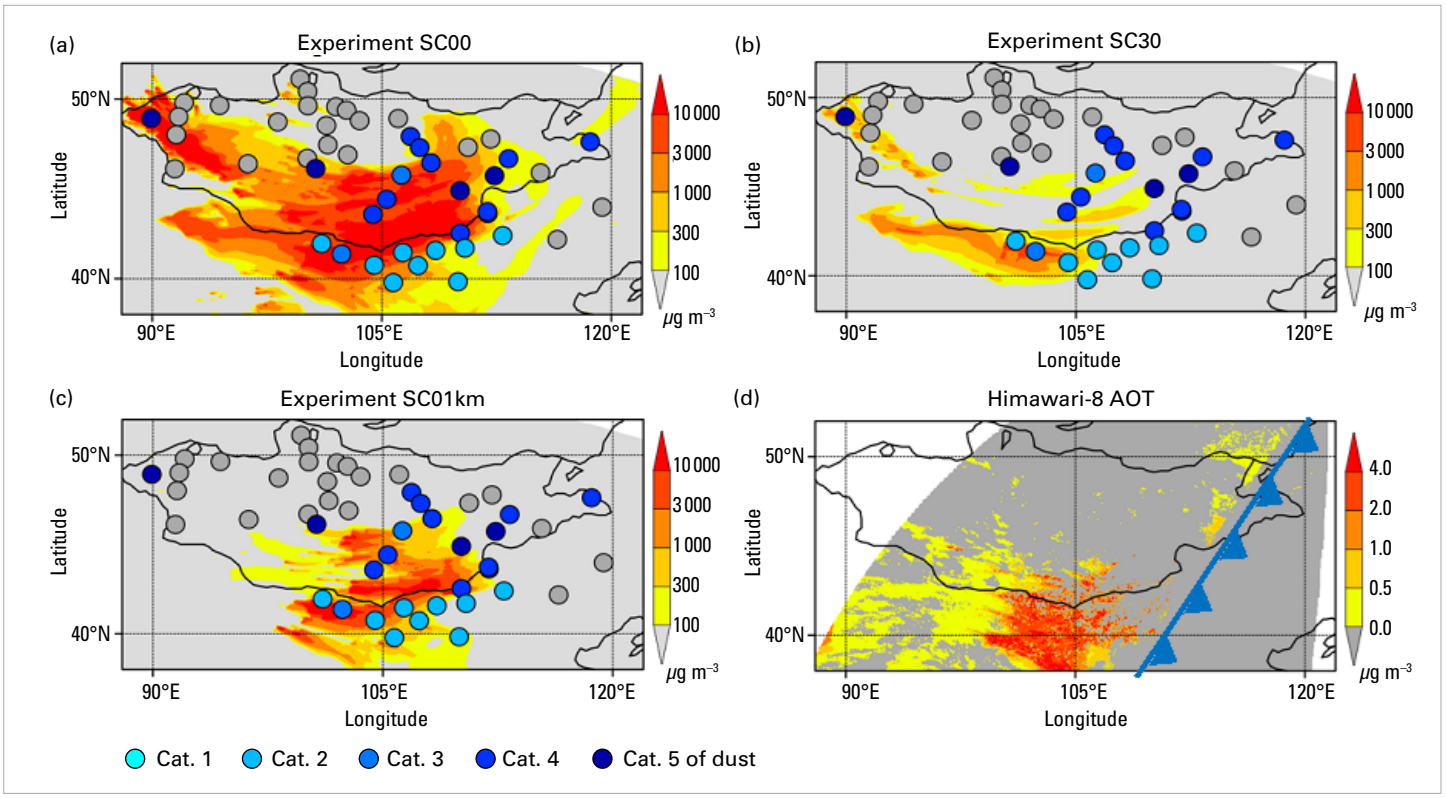

Figure 10. Modelled surface dust concentrations (μg m^{-3}) and SYNOP observatory dust reports (blue circles) at 0900 UTC on 3 May 2017 for (a) the stone-free experiment, (b) the 30% uniform stone-coverage experiment, and (c) the 1 km gridded stone coverage experiment. The 30% stone coverage is the average for the Gobi Desert. The gray circles indicate the observatories that reported anything but dust events. (d) The aerosol optical thickness observation from the Himawari-8 satellite at the same time with the approximate location of the cold front.

Source: This figure is taken from Sekiyama et al. (2023)

weather stations in China and Mongolia (Figure 10). In addition, satellite measurements for air pollution also supported these observations and simulation results. This study is the first successful investigation of the stony surface effects on dust storm simulations using a realistic stone coverage map.

Seasonal dust forecasting

The Korea Meteorological Administration (KMA) has incorporated a sand and dust emission process into its operational climate prediction model (the Global Seasonal Forecasting model version, GloSea6). Since August 2022, KMA has been operating a real-time system for calculating dust PM_{10} concentrations, which are taken into account in Asian dust forecasts. In 2023, using the model's output, KMA produced information for Asian seasonal dust forecasting in the Republic of Korea during spring, categorizing it as "above normal", "near normal" and "below normal" compared to the mean value of the GloSea6's climate period (1993 to 2016). The observed mean number of Asian dust days during the spring of 2023 in the Republic of Korea was 19, placing it in the "above normal" category. The predicted value was 9.78, also falling into the "above normal" category. The spatial pattern of the predicted data indicates an increase in the number of Asian dust days in the southern region of the Republic of Korea, with most areas classified as "above normal", consistent with the observed results (Figure 11). This outcome verifies the capability of GloSea6 in generating output to produce information for Asian dust seasonal forecasting in spring. KMA has established the capability to perform Asian seasonal dust forecasting at any time by continuously producing Asian dust forecast information.

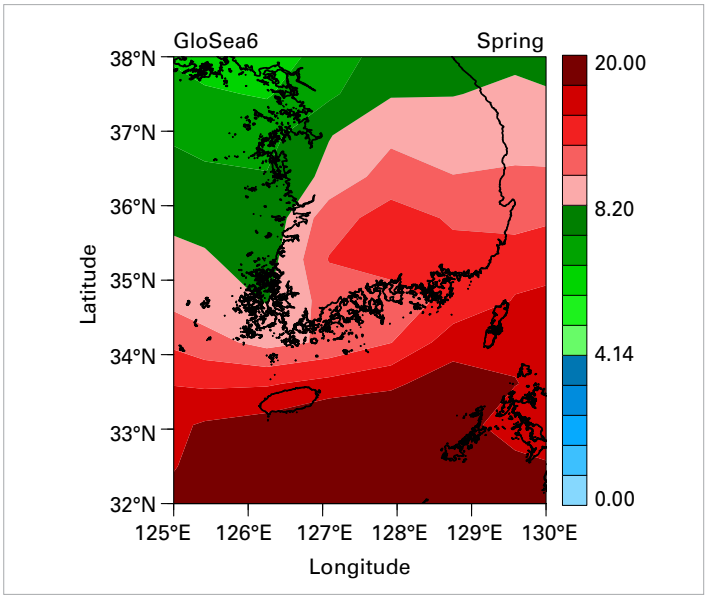

Figure 11. Spatial distribution of predicted Asian dust days in the Republic of Korea for the spring of 2023. The three contour colours represent three categories for Asian seasonal dust forecasting: "above normal" (red), "near normal" (green) and "below normal" (blue).

Dust within the Earth system: dust and ocean interactions

A new study (Rodríguez et al., 2023) found that Saharan dust deposition in the open waters of the Atlantic influences skipjack tuna (*Katsuwonus pelamis*) fisheries. Deposition of desert dust in the open ocean provides iron, phosphorus and biorelevant trace elements that favour the growth of phytoplankton. The resulting new organic matter is transferred across the food web, from small fishes to large predators, favouring the whole marine ecosystem. The role of dust is important for the international management of fisheries. From the 1950s to the 2020s, yearly catches of Atlantic skipjack have increased from less than 1 000 tonnes to average levels of 250 000 tonnes. During the 1990s and 2000s skipjack catches were ~8 times higher in the eastern than in the western Atlantic. Indeed, in the last decade catches in the eastern Atlantic have accounted for ~89% of total Atlantic catches (Figure 12), data that highlight the large skipjack biomass off Western Africa, supported by dust fertilization.

The multiparty 4D-Atlantic Dust-Ocean Modelling & Observing Study (DOMOS) delivered a new satellite-based dataset that contains data on dust optical depth and dust deposition over the Atlantic basin for the period 2007–2020 (Figure 13) and has been evaluated against

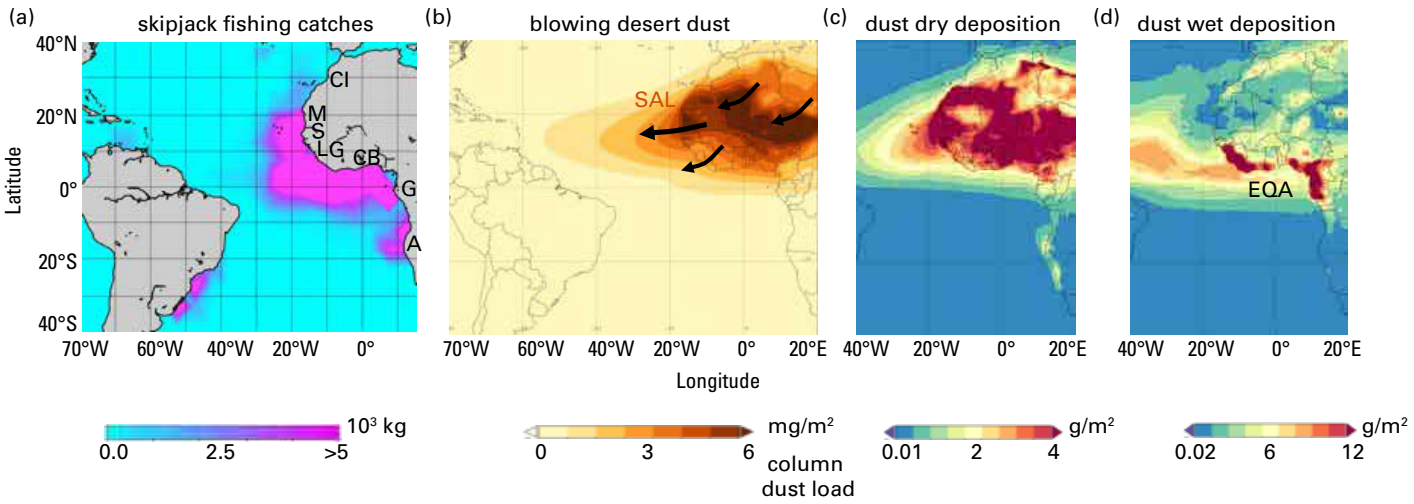

Figure 12. Spatial distribution of average (a) skipjack fishing catches according to International Commission for the Conservation of Atlantic Tunas (ICCAT) data; (b) dust load in the atmospheric column based on MERRA-2 reanalysis, highlighting the dusty airstream of the Saharan air layer (SAL); (c) dry deposition of atmospheric dust accumulated over 1 year based on MERRA-2 reanalysis; (d) wet deposition of atmospheric dust accumulated over 1 year according to MERRA-2 reanalysis

Source: Extracted from Rodríguez et al. (2023)

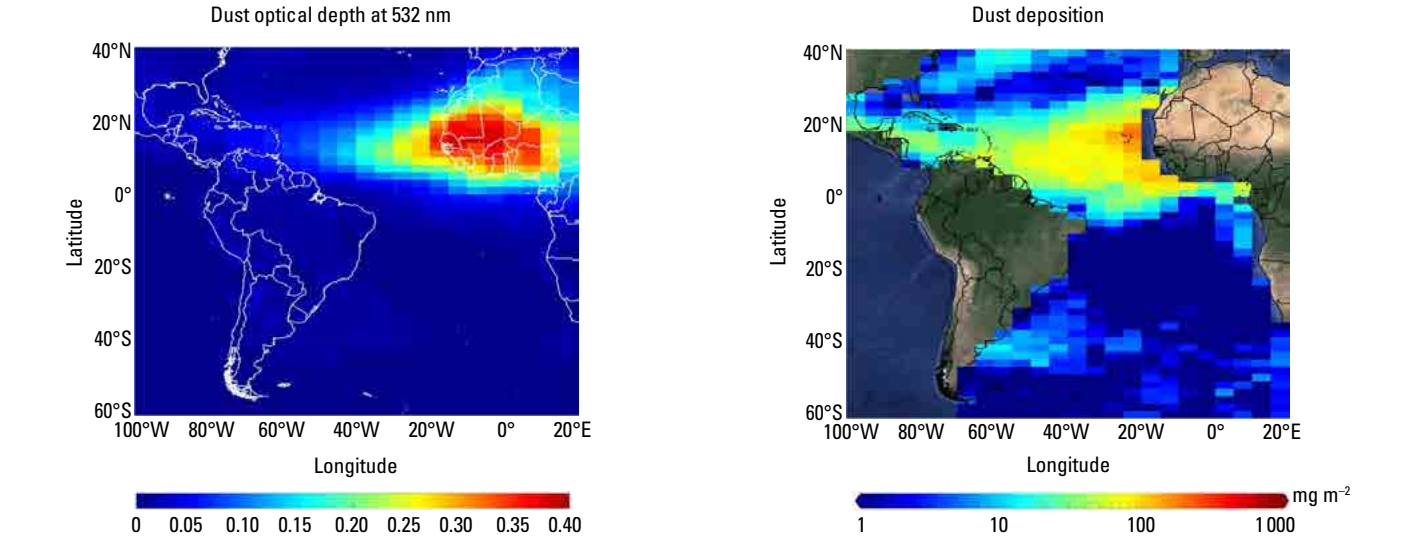

Figure 13. Observations over the Atlantic. Annual mean dust AOD at 532 nm (left) and DOMOS dust deposition rate product (right) for the period 2007–2020.

Source: Emmanouil Proestakis (NOA)

existing deposition datasets. The new DOMOS deposition dataset shows an overestimation compared to the sparse ground-based measurements. This is possibly the result of assumptions that are made regarding dust particle size and scattering properties. These new sets of observed deposition data are used to support studies related to the dust cycle and its connections with atmospheric processes as well as ocean biogeochemistry. A modelled reconstruction of dust and iron deposition from the EC-Earth3-Iron model for the period 1991–2020 was used to study the ocean response to changes in iron sources. Dust remains the most important iron source, with fossil fuel becoming more important over the years, particularly in winter, as well as biomass burning. The use of new dust and iron deposition datasets in an ocean biogeochemistry model showed that the phytoplankton primary production is not increased where the deposition is higher, contrary to what was expected. However, there is an overall increase in iron storage within the ocean, which could affect the seasonality of the phytoplankton primary production and therefore modify the climate feedback from the ocean.

More observations, such as the upcoming EarthCARE and Aeolus lidar observations, are needed to produce more accurate and timely deposition products. DOMOS showed the need for independent observations for the evaluation of satellite-derived products. Moored buoys and ship observations in open ocean areas are key to this calibration and evaluation activity, as they are deployed in areas where ground-based reference measurements are scarce.

Other news

New SDS-WAS Gulf Cooperation Council (GCC) Regional Node

In 2023, WMO SDS-WAS welcomed the Gulf Cooperation Council (GCC) Regional Node and its associated Regional Center in Jeddah (Figure 14). The Jeddah Regional Center is hosted by the National Center for Meteorology of Saudi Arabia. The Regional Node represents six countries in the region (Bahrain, Saudi Arabia, Kuwait, Oman, Qatar and United Arab Emirates), and Jumaan Al-Qahtani (Saudi Arabia) is its Chair. The WMO SDS-WAS GCC Regional Node is promoting capacity building in the region providing a platform to gather and unite experts, scientists and policymakers under a common goal. Promoting regional collaboration will progressively build a path toward sustainable solutions and enhanced regional resilience in the region.

Figure 14. SDS-WAS Gulf Cooperation Council (GCC) Regional Steering Group

Source: National Center for Meteorology, Saudi Arabia

Upgrade for Barbados Atmospheric Chemistry Observatory (BACO)

The University of Miami's Barbados Atmospheric Chemistry Observatory (BACO) was established at Ragged Point, Barbados in 1971 by Professor Emeritus Joseph Prospero. However, dust has been measured on the southeast coast of the island since the 1960s, when Prospero and Toby Carlson discovered that Saharan dust was transported across the Atlantic in the trade winds. Recently, Dr Cassandra Gaston, an atmospheric chemist at the University of Miami's Rosenstiel School of Marine, Atmospheric, and Earth Science, which now manages BACO, acquired a USD 1 million National Science Foundation (NSF) grant to refurbish the site (https://globalmiamimagazine.com/rebirth-for-barbados-observatory/). The upgrade of the facility has included replacing the 3.5 story tower and procuring new instrumentation such as a monitor for trace metals and an aerosol chemical speciation device. The revamped facility (Figure 15) will allow enhanced measurement of indicators of pollution such as particulate matter, smoke, black carbon and ocean emissions, which will lead to improvements in atmospheric models.

Figure 15. Dismantling the old tower (left) and Dr Gaston at the top of the newly erected replacement tower (right) in late January 2024

Source: Caribbean Institute for Meteorology and Hydrology (CIMH)/ University of Miami

International Day of Combating Sand and Dust Storms, 12 July

On 12 July, the world commemorates the first International Day of Combating Sand and Dust Storms, which aims to raise global awareness of the growing health and environmental challenges posed by SDSs. The commemoration follows the adoption of a resolution by the United Nations General Assembly on 8 June 2023.

The first celebration of this international day included an event co-organized by the Permanent Missions of Iraq, the Islamic Republic of Iran and Senegal at the United Nations in New York, featuring various speakers from organizations collaborating in the United Nations Coalition on Combating Sand and Dust Storms. Partners of the Coalition promoted events held around the world to highlight the urgency of this environmental crisis, largely caused by human-induced climate change, desertification, land degradation and drought. w**four WMO SDS-WAS Regional Nodes** hosted a series of regional webinars bringing together stakeholders from different regions.

References

Cuevas-Agulló, E.; Barriopedro, D.; García, R. D. et al. Sharp Increase in Saharan Dust Intrusions over the Western Euro-Mediterranean in February–March 2020–2022 and Associated Atmospheric Circulation. *Atmospheric Chemistry and Physics* **2024**, *24* (7), 4083–4104. https://doi.org/10.5194/acp-24-4083-2024.

Escribano, J.; Di Tomaso, E.; Jorba, O. et al. Assimilating Spaceborne Lidar Dust Extinction Can Improve Dust Forecasts. *Atmospheric Chemistry and Physics* **2022**, *22* (1), 535–560. https://doi.org/10.5194/acp-22-535-2022.

Gelaro, R.; McCarty, W.; Suárez, M. J. et al. The Modern-Era Retrospective Analysis for Research and Applications, Version 2 (MERRA-2). **2017**. https://doi.org/10.1175/JCLI-D-16-0758.1.

Klose, M.; Jorba, O.; Gonçalves Ageitos, M. et al. Mineral Dust Cycle in the Multiscale Online Nonhydrostatic AtmospheRe CHemistry Model (MONARCH) Version 2.0. *Geoscientific Model Development* **2021**, *14* (10), 6403–6444. https://doi.org/10.5194/gmd-14-6403-2021.

Liu, L.; Wang, Z.; Che, H. et al. Climate Factors Influencing Springtime Dust Activities over Northern East Asia in 2021 and 2023. *Atmospheric Research* **2024**, *303*, 107342. https://doi.org/10.1016/j.atmosres.2024.107342.

Prospero, J. M.; Collard, F.-X.; Molinié, J. et al. Characterizing the Annual Cycle of African Dust Transport to the Caribbean Basin and South America and Its Impact on the Environment and Air Quality. *Global Biogeochemical Cycles* **2014**, *28* (7), 757–773. https://doi.org/10.1002/2013GB004802.

Rodríguez, S.; Riera, R.; Fonteneau, A. et al. African Desert Dust Influences Migrations and Fisheries of the Atlantic Skipjack-Tuna. *Atmospheric Environment* **2023**, *312*, 120022. https://doi.org/10.1016/j.atmosenv.2023.120022.

Sekiyama, T. T.; Kurosaki, Y.; Kajino, M. et al. Improvement in Dust Storm Simulation by Considering Stone Coverage Effects for Stony Deserts in East Asia. *Journal of Geophysical Research: Atmospheres* **2023**, *128* (2), e2022JD037295. https://doi.org/10.1029/2022JD037295.

World Meteorological Organization (WMO). *State of the Climate in Asia 2022* (WMO No. 1321). Geneva, 2023.

World Meteorological Organization (WMO). *WMO Airborne Dust Bulletin*, No. 7; WMO: Geneva, 2023.

Zuidema, P.; Alvarez, C.; Kramer, S. J. et al. Is Summer African Dust Arriving Earlier to Barbados? The Updated Long-Term In Situ Dust Mass Concentration Time Series from Ragged Point, Barbados, and Miami, Florida. *Bulletin of the American Meteorological Society* **2019**, *100* (10), 1981–1986. https://doi.org/10.1175/BAMS-D-18-0083.1.

WMO SDS-WAS websites and contacts

WMO SDS-WAS:
https://community.wmo.int/en/activity-areas/gaw/science-for-services/sds-was
Email: gaw@wmo.int

Regional Centre for Northern Africa, Middle East and Europe (NAMEE):
http://dust.aemet.es Email: dust@aemet.es

Regional Centre for Asia:
http://www.asdf-bj.net/ Email: xiaoye@cma.gov.cn

Regional Centre for the Americas:
http://sds-was.cimh.edu.bb/ Email: asealy@cimh.edu.bb

Regional Centre for Gulf Cooperation Council (GCC) Countries:
http://dust.ncm.gov.sa/ Email: sdsc@ncm.gov.sa

Editorial Board

Andrea Sealy (Caribbean Institute for Meteorology and Hydrology (CIMH)), Daniel Tong (George Mason University), Xiaoye Zhang (Chinese Academy of Meteorological Sciences (CMA)), Slobodan Nickovic (Republic Hydrometeorological Service of Serbia), Ana Vuković Vimić (University of Belgrade), Takashi Maki (Meteorological Research Institute, Japan Meteorological Agency (JMA)), Jumaan Saad Alqahtani (National Center for Meteorology (NCM)) and Sara Basart (WMO)

All authors (in alphabetical order)

Melanie Ades, Belghaith Al Moaidi, Sara Attarchi, Rebecca Chewitt-Lucas, Thierry Elias, Emanuelle Emili, David Farrell, Johannes Flemming, Gerardo García-Castrillo, Cassandra Gaston, Hyun-Suk Kang, Saviz Sehat Kashani, Gui Ke, Lin Liu, Alaa Mhaswish, Huiqiong Ning, Mehdi Rahnama, Samuel Remy, Lu Ren, Ashford Reyes, Sergio Rodríguez, Tsuyoshi Thomas Sekiyama, Hong Wang, Yaqiang Wang, Zhili Wang, Ernest Werner

World Meteorological Organization
https://wmo.int/

JN 24859